

Influence of fish scale Biomimetic structure on energy performance of a tidal current turbine

Xingyu Jia, Yan Liu, Cui Wang, Wankun Wang, Yangping Lu and Lei Tan

Abstract—The hydrodynamic performance of the blade is critical to the power generation of a tidal current turbine. Inspired by the surface morphology of fish skin, this study develops a biomimetic blade structure to enhance energy capture efficiency. Key geometric features were extracted from fish scales to design a novel surface texture. A design for a deformable blade, capable of transitioning between a smooth and a textured state via a hydraulic control system, is proposed to optimize performance across a wide range of tip speed ratios (TSRs). The influence of the biomimetic structure on the turbine's energy performance was investigated using computational fluid dynamics (CFD) simulations. Analysis of blade surface shear stress, velocity fields, and pressure distributions reveals the underlying mechanism for the performance improvement. The results show that the concave biomimetic structure increases energy capture efficiency by up to 79.24% under low-CSR conditions.

Keywords—Tidal current turbine, Energy performance, Biomimetic structure, Numerical simulation, Optimization design

I. INTRODUCTION

In recent years, tidal energy generation technology has become an important aspect of marine energy research. Rotational mechanical energy of the turbine is generated by the turbine blades of horizontal axis tidal turbines from the kinetic energy of seawater. Improving the efficiency and stability of turbine blades has consistently been a primary focus and challenge in tidal energy generation [1]. The actual operating conditions of the blades are complex and variable because of the constant variability of ocean currents on the seabed [2]. Under low tip speed ratio (CSR) conditions, in particular, the energy capture efficiency of

conventional blades is often compromised due to complex flow phenomena, such as flow separation on the blade surface.

Horizontal axis tidal turbine blade design is primarily based on Blade Element Momentum (BEM) theory [3]. After obtaining the initial model, it is possible to improve the energy capture efficiency of the blades by optimizing parameters such as blade chord length [4], twist angle [5], and thickness [6]. Different CSR regions can have their energy capture efficiency improved by using various surrogate models and optimization algorithms. Zhu et al. [7] used an artificial neural network model and multi-objective optimization algorithm to adjust the pitch angle and chord length of the blades and increase the highest power factor by 2%, achieving optimal power coefficients within the CSR range of 4 to 6. However, this modification resulted in a slight decrease in the power coefficient at higher CSRs. The lifting surface method and free vortex model were employed by Shen et al. [8], and the blade geometry was optimized using a micro-genetic algorithm. By shortening the chord length, the rotational inertia of the blades was reduced and more than 66% of reduction of the rotor thrust compared with the reference blade, and by increasing the twist angle, the blades generated higher torque, thereby improving the starting performance and energy capture efficiency in the low-CSR region. However, this optimization resulted in decreased rotor thrust and annual energy production. Cresswell et al. [9] used a Kriging surrogate model and genetic algorithm to optimize the geometry of the diffuser, increasing the momentum of the flow within the boundary layer, allowing the turbine blades to maintain near-peak performance even at yaw angles up to $\pm 30^\circ$. The optimized diffuser contributed to a decrease in wake recovery effect. Therefore, further research is necessary to enhance wake

Part of a special issue for AWTEC 2024. Manuscript submitted 17 November 2024; Revised 20 September 2025; Accepted 13 October 2025. Published 20 October 2025.

This is an open access article distributed under the terms of the Creative Commons Attribution 4.0 International license. CC BY <https://creativecommons.org/licenses/by/4.0/>. Unrestricted use (including commercial), distribution and reproduction is permitted provided that credit is given to the original author(s) of the work, including a URI or hyperlink to the work, this public license and a

copy right notice. This article has been subject to a single-blind peer review by a minimum of two reviewers.

Corresponding author, Lei Tan, is at the Department of Energy and Power Engineering, Tsinghua University, Beijing, China, e-mail: tanlei@mail.tsinghua.edu.cn.

X. Jia, Y. Lu and L. Tan were at the Department of Energy and Power Engineering, Tsinghua University, Beijing, China.

Y. Liu, C. Wang, W. Wang were at the China Datang Technology Innovation. Corp., Hebei, China.

Digital Object Identifier: <https://doi.org/10.36688/imej.8.389-394>

mixing to improve the performance of turbine blade arrays after deployment.

In addition to achieving passive control of the flow state by adjusting the geometric parameters of the blade airfoil, active control methods can further control the flow state on the blade surface, improving the energy capture efficiency of the horizontal axis tidal turbine blades under various operating conditions. Wang et al. [10] employed a variable pitch technique to enable the turbine to attain its maximum output torque at various current speeds, thereby achieving the optimal operating point. Manolesos et al. [11] were able to effectively reduce flow separation on the blade by adding vortex generators to its surface, which resulted in an enhancement of the turbine's maximum power coefficient by 1.05%.

Marine organisms possess outstanding natural abilities to control surface flow. Biomimetic design has been applied successfully to significantly improve the performance of tidal energy blades at different TSRs. Biomimetic leading-edge tubercles were created by Shi et al. [12] to maintain more attached flow on the blade surface during stall conditions, resulting in additional starting torque for the turbine. And the thrust coefficient is increased by 9.2% at optimum working condition. According to Shi et al. [13], models with leading-edge tubercles are less sensitive to Reynolds number changes, which is because the leading-edge tubercles on the turbine blades cause earlier transition. Fan et al. [14] identified the leading-edge tubercles to be able to eliminate the persistent flow separation on the suction side of the blade, resulting in enhanced energy conversion performance in the Biomimetic structure turbine at lower TSRs. However, it exhibits poor performance at higher TSRs.

The above analysis highlights the complexity of the actual operating conditions of horizontal axis tidal current turbines. Adapting to different incoming flow conditions is challenging for a single blade design method, particularly in the low-performance region with low-TSRs. Current biomimetic structures are predominantly confined to the leading-edge region of blades. Few studies have documented Biomimetic variable structures specifically engineered for tidal current turbines. This study introduces a novel biomimetic design method inspired by fish scale morphology. We propose a deformable blade concept, incorporating a hydraulic control system, which allows the blade surface to transition to a biomimetic texture under low-TSR

TABLE I
DESIGN PARAMETERS OF TIDAL CURRENT TURBINE BLADE

Symbol	Quantity	Unit
V	Rated inflow velocity	3 m/s
N	Rotational speed	1008 rpm
D	Radius of impeller	125 mm
B	Blade number	3
λ	Rated TSR	5
-	Airfoil	NACA 63-821

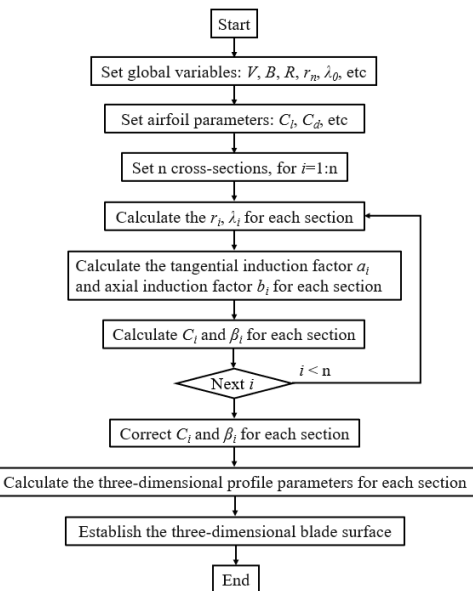


Fig. 1. Design process of the tidal current turbine blade.

conditions. This adaptability aims to maintain high energy capture efficiency across the full operational range of TSRs. Furthermore, the underlying fluid dynamic mechanisms responsible for the performance enhancement are investigated and explained.

II. DESIGN METHOD OF BLADE AND BIOMIMETIC STRUCTURE

The design process of the smooth airfoil form blade is shown in Figure 1. The basic performance parameters of the designed blade are shown in Table I.

Set the global parameters and airfoil data according to the parameter values in Table I. The blades are divided into 9 sections, and the λ_i for each section is determined based on the radius values. The tangential induction factor a_i and axial induction factor b_i for each section are obtained using the Wilson optimization [15]. The chord length C_i and installation angle β_i for each section are then calculated. After modification using the Wilson correction model [16], the spatial airfoil data for each section is



Fig. 2. Fish-scale prototype.

derived based on the NACA airfoil data. Finally, the three-dimensional blade surface is established based on the spatial airfoil data.

Evolved over millions of years, fish scales regulate surface flow through their unique textures and layered arrangements, making them an ideal prototype for biomimetic design. Inspired by this mechanism, as shown in Figure 2, this study integrates a biomimetic scale structure onto the smooth blade surface to enhance the energy capture efficiency of tidal current turbine blades under low TSR conditions.

The geometric parameters that determine the shape of the fish scales, as well as the geometric parameters that determine the relative positions of the scales on the plane, are shown in Figure 3. The structure of a fish scale consists

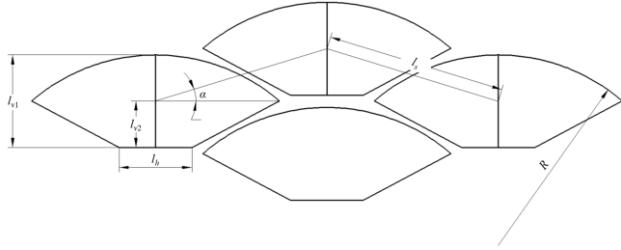


Fig. 3. Biomimetic structure.

TABLE II
LEVEL OF THE ORTHOGONAL EXPERIMENT AND RESULT

level	α (°)	l_h (mm)	l_{v1} (mm)	l_{v2} (mm)	l_s (mm)	R (mm)
1	17	4.0	6.5	3.0	11.0	13.0
2	25	5.0	7.5	4.0	12.0	14.0
3	33	6.0	8.5	5.0	13.0	15.0
Result	17	5.0	6.5	3.0	12.0	13.0

of a leading edge line determined by l_h , a trailing edge curve determined by R , and two symmetrical side edge lines determined by l_{v1} and l_{v2} . These units are aligned with the fluid flow direction across the blade. The fish scale structural units can be arranged according to the angle α and length l_s as shown in Figure 3. Considering the proportional arrangement of fish scales on fish bodies and the area on the blade surface, we designed levels for the above six parameters as shown in Table II and selected an

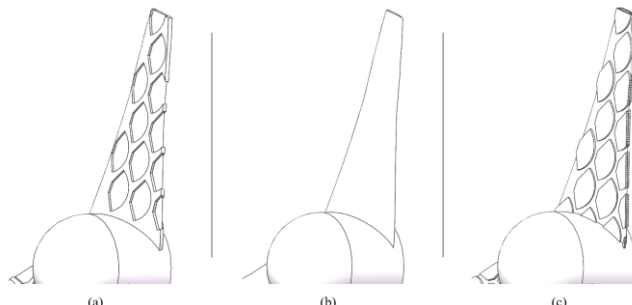


Fig. 4. (a) Blade with the concave Biomimetic structure, (b) smooth airfoil form blade, (c) blade with the convex Biomimetic structure. L18(3⁷) orthogonal experimental design. Using range analysis, we determined the final geometric parameters which are also listed in Table II.

The fish scale structure was arranged on the smooth blade surface as shown in Figure 4. Design the concave fish scale structure in Figure 4(a) and the convex fish scale structure in Figure 4(c) respectively, to explore the impact of the concave and convex Biomimetic forms on the hydraulic performance of the turbine blades. Specifically, the concave Biomimetic structure is recessed 1mm below the smooth blade surface, while the convex Biomimetic structure protrudes 1mm above the smooth blade surface.

III. NUMERICAL SETUPS

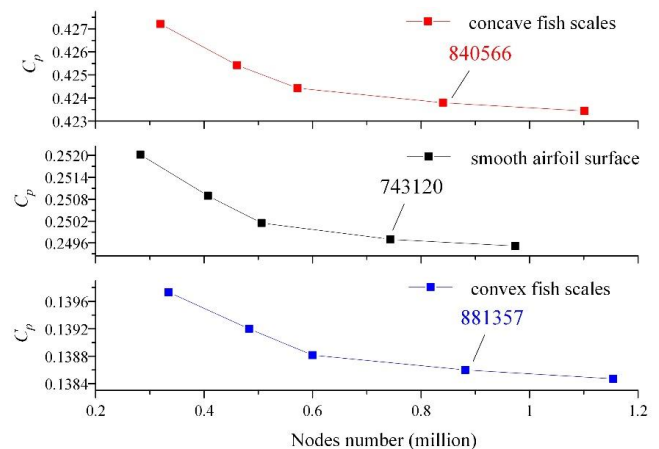


Fig. 5. Grid sensitivity analysis result.

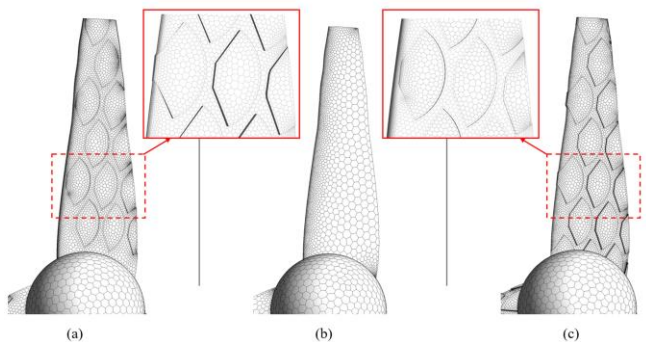


Fig. 6. Grids layout (a) blade with the concave Biomimetic structure, (b) smooth airfoil form blade, (c) blade with the convex Biomimetic structure.

A. Meshing

The essential aspects were identified of every blade model, establish the flow control volume, and discretize the computational domain using a polyhedral mesh [17].

The mesh was refined at the leading and trailing edges of the blades, blade tip and root, and the ridge positions of the Biomimetic structures. A grid independence study was conducted (Figure 5), and the fourth mesh configuration was selected for subsequent simulations. The final node counts for the concave, smooth, and convex models were 840,566, 743,120, and 881,357, respectively. Figure 6 provides an overview of the mesh. The height of the first layer of the grid is calculated according to the requirement of the RNG k - ε turbulence model that $y^+ = 30$. The mesh distribution in the Biomimetic structure area is optimized through the adaptive mesh refinement algorithm.

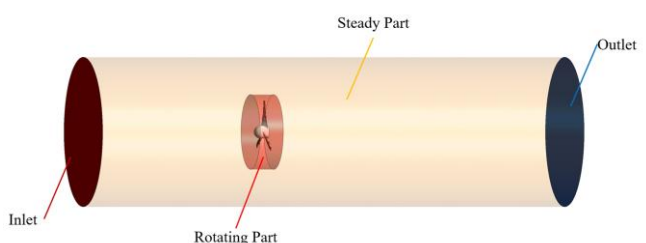


Fig. 7. Computing frames.

B. Numerical technique

The numerical simulations were carried out by the ANSYS-FLUENT solver after dividing the control volumes into unstructured grids. The RNG $k-\varepsilon$ turbulence model, was applied for steady-state simulation (based on Reynolds-averaged Navier-Stokes equations) [18]. The

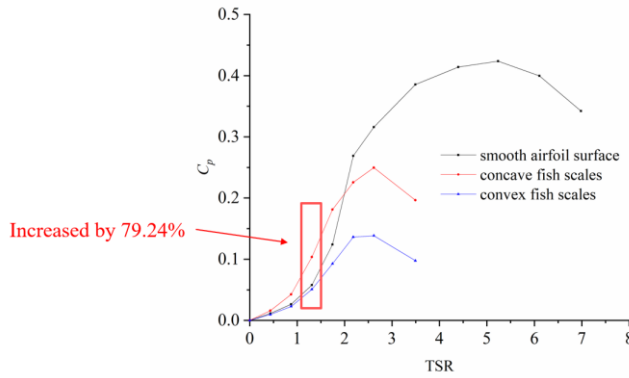


Fig. 8. Effect of Biomimetic structures on the energy capture efficiency curves.

flow medium was the liquid water. The rotating and stationary domains were connected using interfaces, and the Multiple Reference Frame (MRF) approach was employed to simulate blade rotation (Figure 7). The

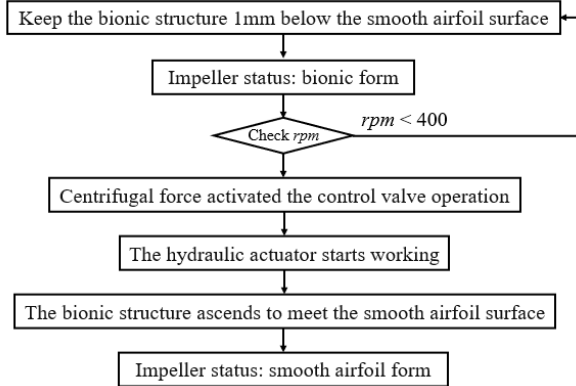


Fig. 9. Deformable blade scheme.

atmospheric (atm) parameters were 298.15 K and 1 atm. The flow was normal to the boundary at a speed of 3 m/s through the inlet. An outflow boundary condition was applied at the domain outlet. A specific operational condition was determined by the speed of rotation. The distance between the inlet and the turbine is 0.7 m. The distance between the outlet and the turbine is 1.2 m.

IV. RESULT

C. Energy capture efficiency curves

Figure 8 illustrates the variation in energy capture efficiency with TSR. In the low-TSR region, the concave Biomimetic structure displays the best performance. The energy capture efficiency increased by 79.24% at 300 rpm. To ensure that the turbine blades maintain high energy capture efficiency under different operating conditions, a deformable blade scheme is proposed, shown in Figure 9.

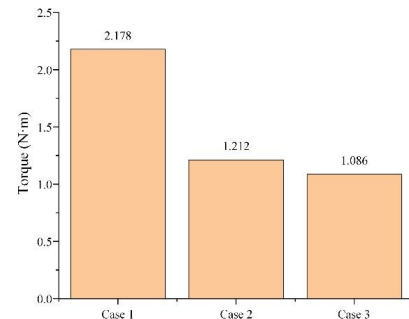


Fig. 10. Comparison of torque for different blades.

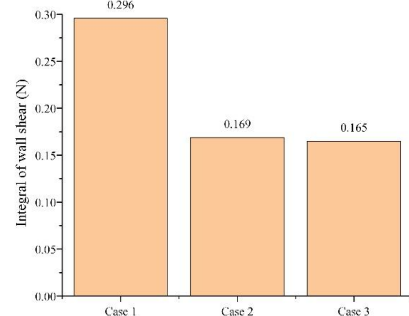


Fig. 11. Comparison of wall shear for different blades.

If the turbine speed is lower than 400 rpm, the blade surface maintains its concave fish scale configuration. When the rotational speed exceeds 400 rpm, the centrifugal force activates a hydraulic control valve. This propels an actuator that elevates the scale elements, filling the grooves and creating a smooth, conventional airfoil surface. This is referred to as the 'smooth airfoil form'.

D. Comparison of torque and wall shear

An increase in torque is critical for improving the starting performance of a turbine at low TSRs [19]. In Figure 10, it can be seen that the torque of the concave fish scale structure is 79.70% greater than the smooth airfoil structure at 300 rpm, under the low-TSR condition. The concave fish scale structure, smooth airfoil blade, and convex fish scale structure are represented by Case 1, Case 2, and Case 3. On the other hand, the integral stress of wall shear on the concave fish scale structure is increased by

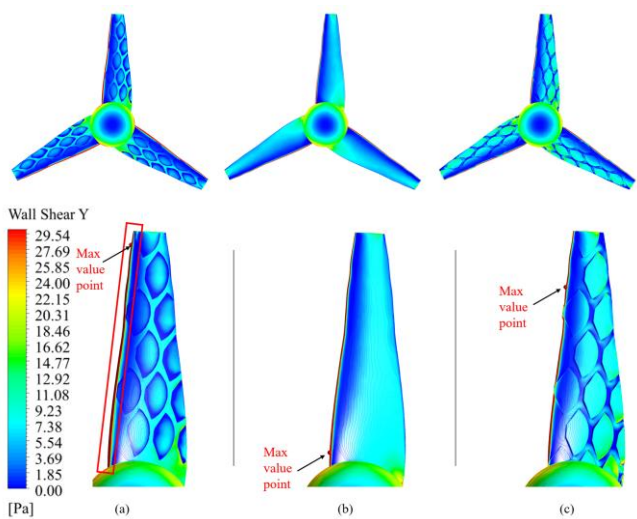


Fig. 12. Comparison of wall shear distribution for different blades (inflow face).

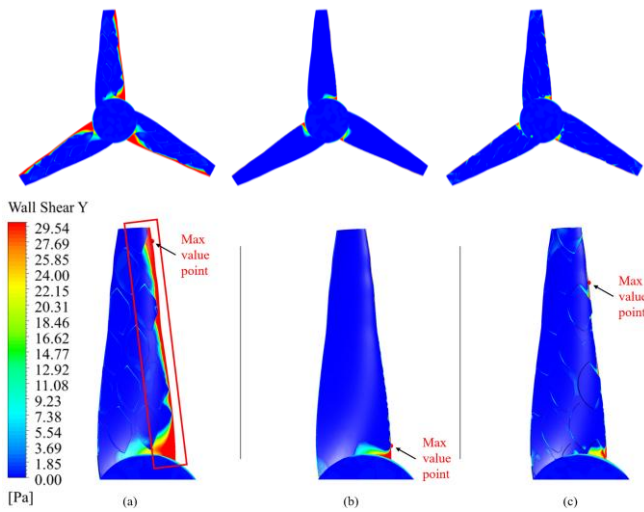


Fig. 13. Comparison of wall shear distribution for different blades (outflow face).

75.15% compared to the smooth airfoil structure, as depicted in Figure 11.

E. Comparison of wall shear distributions

Specifically, by analyzing the wall shear stress distribution of the three blades through surface contours, it can be seen that the maximum shear stress point of the concave fish scale structure is located near the blade tip, which is more conducive to the turbine obtaining torque. Compared with the other two blades, the high wall shear stress area within the red box on the inflow surface (as shown in Figure 12) and the outflow surface (as shown in Figure 13) of the concave fish scale structure is significantly widened.

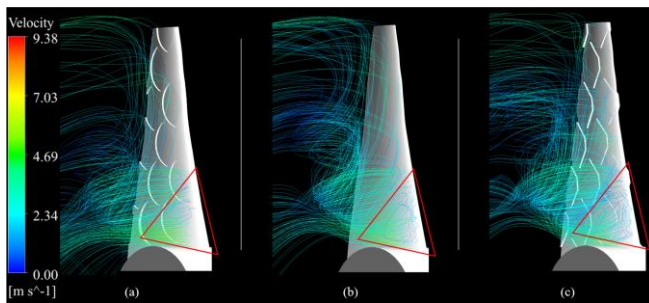


Fig. 14. Comparison of flow patterns for different blades.

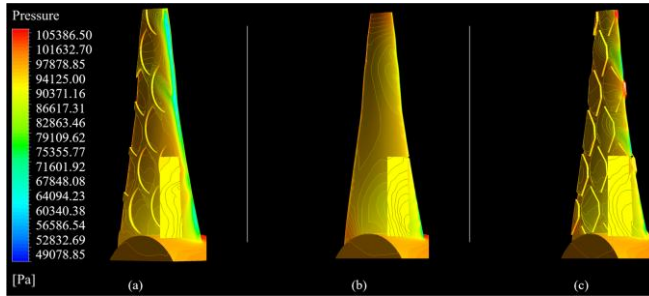


Fig. 15. Comparison of pressure distributions for different blades.

F. Comparison of flow patterns

As highlighted in Figure 14 (red triangle), the concave scale structure mitigates flow separation near the blade root on the suction side, promoting more attached flow.

This increases the effective contact area between the fluid and the blade, enhancing the transfer of kinetic energy to the turbine via viscous forces [20].

G. Comparison of pressure distributions

As illustrated in Figure 15, it can be seen that the fish scale structure effects in the pressure distribution near the blade wall, which reduces the pressure gradient, inhibits the formation of vortices, and prevents flow separation at the blade root.

V. CONCLUSION

Concave and convex Biomimetic structures are designed using the surface structure of fish as inspiration for this paper. Numerical calculations were used to study how Biomimetic structures affect energy capture efficiency, and the following findings were made:

- 1) The concave Biomimetic structure has the capability to enhance the performance of tidal turbine blades in the low-CSR region, but it does not perform well in non-low-CSR regions.
- 2) The concave Biomimetic structure significantly impacts turbine torque by expanding the high wall shear stress distribution area, which is advantageous for enhancing the startup performance of the blades.
- 3) The concave Biomimetic structure can control surface flow by adjusting the pressure distribution on the outflow surface.

In conclusion, the proposed biomimetic surface, combined with a deformable blade strategy, presents a promising approach for designing tidal turbine blades that can achieve high efficiency across a broader range of operating conditions.

REFERENCES

- [1] Z. Yang et al., "A review of tidal current power generation farm planning: Methodologies, characteristics and challenges," in *Renewable Energy*. vol. 220, pp. 119603, 2023. <https://doi.org/10.1016/j.renene.2023.119603>
- [2] M. Nachtane et al., "A review on the technologies, design considerations and numerical models of tidal current turbines," in *Renewable Energy*. vol. 157, pp. 1274-1288, 2020. <https://doi.org/10.1016/j.renene.2020.04.155>
- [3] W. Li et al., "Review on the blade design technologies of tidal current turbine," in *Renewable and Sustainable Energy Reviews*. vol. 63, pp. 414-422, 2016. <https://doi.org/10.1016/j.rser.2016.05.017>
- [4] J. Xu et al., "A cost-effective CNN-BEM coupling framework for design optimization of horizontal axis tidal turbine blades," in *Energy*. vol. 282, pp. 128707, 2023. <https://doi.org/10.1016/j.energy.2023.128707>
- [5] B. Huang and T. Kanemoto, "Multi-objective numerical optimization of the front blade pitch angle distribution in a counter-rotating type horizontal-axis tidal turbine," in *Renewable Energy*. vol. 81, pp. 837-844, 2015. <https://doi.org/10.1016/j.renene.2015.04.008>
- [6] P. M. Kumar et al., "Multi-fidelity optimization of blade thickness parameters for a horizontal axis tidal stream turbine," in *Renewable energy*, vol. 135, pp. 277-287, 2019. <https://doi.org/10.1016/j.renene.2018.12.023>

- [7] F. W. Zhu et al., "Blade design and optimization of a horizontal axis tidal turbine," in *Ocean Engineering*, vol. 195, pp. 106652, 2020. <https://doi.org/10.1016/j.oceaneng.2019.106652>
- [8] X. Shen et al., "Aerodynamic shape optimization of non-straight small wind turbine blades," in *Energy Conversion and Management*, vol. 119, pp. 266-278, 2016. <https://doi.org/10.1016/j.enconman.2016.04.008>
- [9] N. W. Cresswell et al., "The impact of diffuser augmentation on a tidal stream turbine," in *Ocean Engineering*, vol. 108, pp. 155-163, 2015. <https://doi.org/10.1016/j.oceaneng.2015.07.033>
- [10] B. Z. Wang et al., "Research on pitch control strategies of horizontal axis tidal current turbine," in *China Ocean Engineering*, vol. 34, pp. 223-231, 2020. <https://doi.org/10.1007/s13344-020-0021-9>
- [11] M. Manolesos et al., "Using vortex generators for flow separation control on tidal turbine profiles and blades," in *Renewable Energy*, vol. 205, pp. 1025-1039, 2023. <https://doi.org/10.1016/j.renene.2023.02.009>
- [12] W. Shi et al., "Detailed flow measurement of the field around tidal turbines with and without biomimetic leading-edge tubercles," in *Renewable Energy*, vol. 111, pp. 688-707, 2017. <https://doi.org/10.1016/j.renene.2017.04.053>
- [13] W. Shi et al., "Effect of waves on the leading-edge undulated tidal turbines," in *Renewable energy*, vol. 131, pp. 435-447, 2019. <https://doi.org/10.1016/j.renene.2018.07.072>
- [14] M. Fan et al., "Effect of leading-edge tubercles on the hydrodynamic characteristics and wake development of tidal turbines," in *Journal of Fluids and Structures*, vol. 119, pp. 103873, 2023. <https://doi.org/10.1016/j.jfluidstructs.2023.103873>
- [15] J. Chen et al., "Design of the blade under low flow velocity for horizontal axis tidal current turbine," in *Journal of Marine Science and Engineering*, vol. 8, pp. 989, 2020. <https://doi.org/10.3390/jmse8120989>
- [16] H. A. Oliveira et al., "Comparative study of different correction methods to analyze wind turbine performance," presented at the *In 2019 IEEE 15th Brazilian Power Electronics Conference and 5th IEEE Southern Power Electronics Conference*, 2019. <https://doi.org/10.1109/COBEP/SPEC44138.2019.9065754>
- [17] D. M. Martins et al., "On the use of polyhedral unstructured grids with a moving immersed boundary method," in *Computers & Fluids*, vol. 174, pp. 78-88, 2018. <https://doi.org/10.1016/j.compfluid.2018.07.010>
- [18] G. Alfonsi, "Reynolds-averaged Navier-Stokes equations for turbulence modelling" in *Applied Mechanics Reviews*, vol. 62, pp. 040802, 2009. <https://doi.org/10.1115/1.3124648>
- [19] V. Akbari et al., "Multi-objective optimization of a small horizontal-axis wind turbine blade for generating the maximum startup torque at low wind speeds" in *Machines*, vol. 10, pp. 785, 2022. <https://doi.org/10.3390/machines10090785>
- [20] W. G. Li, "Effects of viscosity of fluids on centrifugal pump performance and flow pattern in the impeller," in *International journal of heat and fluid flow*, vol. 21, pp. 207-212, 2000. [https://doi.org/10.1016/S0142-727X\(99\)00078-8](https://doi.org/10.1016/S0142-727X(99)00078-8)